Supporting Information

Dunn et al. 10.1073/pnas.1216514110

SI Materials and Methods

Imaging and Analysis. Artificial cerebral spinal fluid (aCSF) used in brain slice experiments was composed of 125 mM NaCl, 3 mM KCl, 26 mM $NaHCO_3$, 1.25 mM NaH_2PO_4, 2 mM $CaCl_2$, 1 mM $MgCl_2$, 4 mM glucose, and 400 μM L-ascorbate, equilibrated with 95% O_2/5% CO_2 to pH 7.4. The acute effects of transient receptor potential vanilloid 4 (TRPV4) channel activation on endfoot Ca^{2+} and arteriolar diameter were evaluated by exposing brain slices to the synthetic TRPV4 agonist, GSK1016790A (100 nM), and the endogenous TRPV4 agonist, 11,12-EET (epoxyeicosatrienoic acid) (1 μM). Images were continuously recorded as the bath perfusate was switched from normal aCSF to aCSF containing the TRPV4 agonist. Endfoot Ca^{2+} and arteriolar diameter were continuously recorded for 5 min after the drug entered the bath (time to equilibrium, ~2 min). Slices were preincubated with the TRPV4 antagonist, HC-067047 (1 μM), for 25 min before application of GSK1016790A and 11,12-EET.

Endfoot Ca^{2+} events and parenchymal arteriole diameter data obtained from brain slices were analyzed using custom software designed by A. Bonev (University of Vermont). Fractional fluorescence ($\Delta F/F_o$) values reflect the fluorescence intensity for a region of interest (ROI; 8 pixels × 8 pixels, or 1 × 1 μm) in each image (F) divided by a mean fluorescence value taken from 20 to 50 images before stimulation (F_o). The brain slice preparation exhibits slightly higher basal noise during fluorescence imaging than do other tissues and preparations due to its complex 3D architecture. Taking into account the SD of basal fluorescence signals in the brain slice preparation using our multiphoton imaging system, fractional fluorescence changes ≥0.3 $\Delta F/F_o$ were considered real events above baseline noise. ROIs were placed throughout the entire visible area of the endfoot, and the frequency of events before and after treatment was obtained by identifying oscillations that were ≥0.3 $\Delta F/F_o$. Maximum amplitude observed after treatment was compared with maximum amplitude observed during baseline, regardless of whether the amplitude met the criterion for an event (≥0.3 $\Delta F/F_o$). The spatial spread of Ca^{2+} oscillations was obtained by measuring the full linear width of the oscillation at ≥0.3 $\Delta F/F_o$.

Astrocytic endfoot Ca^{2+} concentrations were estimated using the maximal fluorescence method described in detail previously (1–3). A maximum fluorescence intensity (F_{max}) was obtained by adding the Ca^{2+} ionophore, ionomycin (10 μM), and 20 mM external Ca^{2+} to the slice. An estimate of $[Ca^{2+}]_i$ is obtained for a fluorescence intensity (F) from a ROI placed within the endfoot using the equation:

$$Ca^{2+} = K_d \frac{F/F_{max} - 1/Rf}{1 - F/F_{max}},$$

where K_d is the Fluo-4 AM dissociation constant (340 nM) and R*f* is the ratio of Fluo-4 AM fluorescence in vitro at saturation relative to 0 $[Ca^{2+}]$ (=100) (4).

Neuronal Activation by Electrical Field Stimulation in Brain Slices. Neurovascular coupling (NVC) in brain slices was examined using electrical field stimulation (EFS) to stimulate neurons (2). A 50-Hz alternating square pulse of 0.3-ms duration (10–20 V) was applied to the brain slice for 3 s through a pair of platinum wires positioned immediately above and parallel to the slice, straddling the neurovascular unit to be imaged. When functional coupling of neurons and astrocytes is intact, EFS produces a rise in astrocytic endfoot Ca^{2+}. Astrocytic endfeet in which fluorescence did not increase in response to EFS were not studied. Pharmacological effects on NVC were determined in paired experiments measuring endfoot Ca^{2+} and arteriolar diameter in response to EFS before and after incubation of the slice with the drug.

In Vivo Cerebral Blood Flow Measurement. Cerebral hemodynamics in the somatosensory cortex were measured using laser Doppler flowmetry in a mouse cranial window model, as previously described (5, 6). Surgical plane anesthesia was induced with brief exposure to 5.0% isoflurane and maintained with 2.0% isoflurane. Isoflurane was discontinued at the conclusion of surgical preparation. Mice were given chloralose (50 mg/kg, i.p.) and urethane (750 mg/kg, i.p.) for maintenance of anesthesia after withdrawal of isoflurane. Body temperature was recorded with a rectal probe and maintained at 37 °C by a servo-controlled heating pad. Animals were instrumented with a femoral arterial catheter for mean arterial pressure recording and arterial blood gas measurement, and an endotracheal catheter for mechanical ventilation (SAR-830; CWE Inc.). After immobilization of the head in a stereotaxic frame, the cisterna magna was punctured to relieve CSF pressure, a 2 × 2 mm craniotomy was performed over the somatosensory cortex, and the underlying dura was slit open. The cranial window was superfused with aCSF composed of 125 mM NaCl, 3 mM KCl, 26 mM $NaHCO_3$, 1.25 mM NaH_2PO_4, 2 mM $CaCl_2$, 1 mM $MgCl_2$, and 4 mM glucose. Throughout the experiment, the depth of anesthesia was assessed by monitoring blood pressure and reflex responses to tail pinch. A laser Doppler flow probe (Perimed) was placed over the cranial window for cerebral blood flow (CBF) measurement. CBF is recorded in arbitrary perfusion units (P.U.). Arterial pressure and CBF were recorded using computerized data-acquisition software (PowerLab; AD Instruments). CBF and mean arterial pressure were allowed to stabilize for 30 min before experimental intervention. NVC was assessed by stimulating contralateral whiskers (cut to 10 mm length) using a piezoelectric actuator driven by a programmable waveform generator coupled to an amplifier (Piezo Master; Viking Industrial Products) (7). Whiskers were deflected at a frequency of 4 Hz for 1 min with a total deflection of 4 mm. Drugs were delivered locally via the cranial window superfusate. The CBF response to whisker stimulation was quantified by calculating total area under the curve of the CBF trace during the 60 s stimulus using Prism 6 software (GraphPad Software, Inc.). The effect of TRPV4 inhibition on resting CBF was assessed following superfusion of the selective TRPV4 antagonist HC-067047 (10 μM) for 25 min. CBF responses to whisker stimulation were obtained before and after cortical application of HC-067047.

Reagents. GSK1016790A was obtained from Sigma-Aldrich. GSK1016790A has been demonstrated to have nanomolar potency for activating TRPV4, with half activation at 18 nM for mouse TRPV4 (8). This compound does not activate other transient receptor potential channel subfamily members at micromolar concentrations. HC-067047 was kindly provided by Hydra Biosciences, Inc. HC-067047 is a potent and highly selective TRPV4 antagonist, with an IC_{50} of 17 nM for mouse TRPV4; it has no effect on Ca^{2+} influx through TRPV1, TRPV3, or other members of the TRPM (melastatin), TRPA (ankyrin), or TRPC (canonical) subfamilies at micromolar concentrations (9). The 11,12-EET was purchased from Cayman. The sarcoplasmic reticulum (SR)/endoplasmic reticulum (ER) Ca^{2+} ATPase inhibitor, cyclopiazonic acid (CPA), was obtained from Calbiochem. Fluo-4 AM and pluronic acid were purchased from Invitrogen.

1. Maravall M, Mainen ZF, Sabatini BL, Svoboda K (2000) Estimating intracellular calcium concentrations and buffering without wavelength ratioing. *Biophys J* 78(5): 2655–2667.
2. Girouard H, et al. (2010) Astrocytic endfoot Ca2+ and BK channels determine both arteriolar dilation and constriction. *Proc Natl Acad Sci USA* 107(8):3811–3816.
3. Koide M, Bonev AD, Nelson MT, Wellman GC (2012) Inversion of neurovascular coupling by subarachnoid blood depends on large-conductance Ca2+-activated K+ (BK) channels. *Proc Natl Acad Sci USA* 109(21):E1387–E1395.
4. Woodruff ML, et al. (2002) Measurement of cytoplasmic calcium concentration in the rods of wild-type and transducin knock-out mice. *J Physiol* 542(Pt 3): 843–854.
5. Niwa K, Araki E, Morham SG, Ross ME, Iadecola C (2000) Cyclooxygenase-2 contributes to functional hyperemia in whisker-barrel cortex. *J Neurosci* 20(2):763–770.
6. Longden TA, et al. (2011) Intermediate-conductance calcium-activated potassium channels participate in neurovascular coupling. *Br J Pharmacol* 164(3):922–933.
7. Andermann ML, Ritt J, Neimark MA, Moore CI (2004) Neural correlates of vibrissa resonance; band-pass and somatotopic representation of high-frequency stimuli. *Neuron* 42(3):451–463.
8. Thorneloe KS, et al. (2008) N-((1S)-1-[4-((2S)-2-[(2,4-dichlorophenyl)sulfonyl]amino-3-hydroxypropanoyl)-1-piperazinyl]carbonyl-3-methylbutyl)-1-benzothiophene-2-carboxamide (GSK1016790A), a novel and potent transient receptor potential vanilloid 4 channel agonist induces urinary bladder contraction and hyperactivity: Part I. *J Pharmacol Exp Ther* 326(2):432–442.
9. Everaerts W, et al. (2010) Inhibition of the cation channel TRPV4 improves bladder function in mice and rats with cyclophosphamide-induced cystitis. *Proc Natl Acad Sci USA* 107(44):19084–19089.

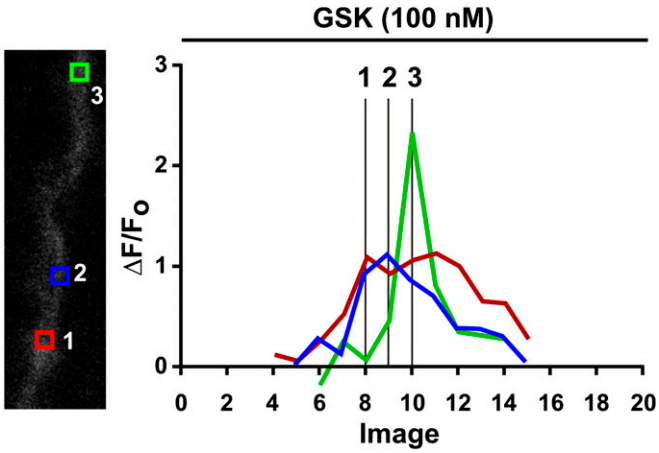

Fig. S1. TRPV4 channel activation stimulates Ca^{2+} waves in astrocytic endfeet. The endfoot Ca^{2+} event elicited by GSK (100 nM) depicted in Fig. 1*B* did not decrease in amplitude as it propagated from its origin at ROI 1 (red) to ROI 2 (blue) and then ROI 3 (green), where it terminated. The nondecremental, propagating characteristics identify this Ca^{2+} event as a Ca^{2+} wave, as opposed to diffusional spread of Ca^{2+} from a stationary event.

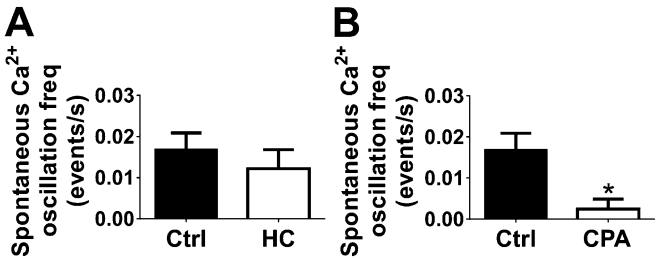

Fig. S2. Spontaneous Ca^{2+} oscillations in astrocytic endfeet are independent of TRPV4 channel activity. (*A*) The frequency of spontaneous Ca^{2+} oscillations in unstimulated endfeet was unaffected by HC-067047 (10 μM; $n = 16$ for Control; $n = 9$ for HC). (*B*) Spontaneous endfoot Ca^{2+} oscillations were nearly eliminated by incubation with CPA ($P < 0.05$; $n = 16$ for Control; $n = 5$ for CPA). Values were compared by unpaired *t* test.

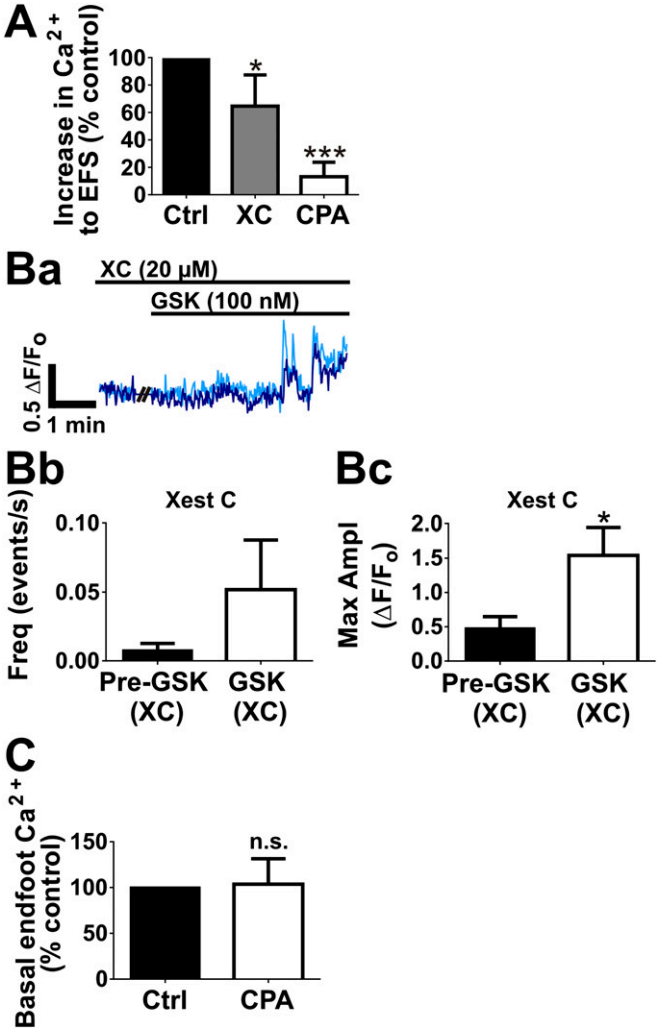

Fig. S3. Partial inhibition of inositol 1,4,5-trisphosphate (IP_3) receptor Ca^{2+} release channels (IP_3R) in brain slices by xestospongin C (XC) further supports the triggering of IP_3R Ca^{2+} release by TRPV4 channel activation. (*A*) (20 μM) is only partially effective at blocking IP_3Rs in brain slices, reducing the rise in endfoot Ca^{2+} to EFS to 64% ± 11% of control ($P < 0.05$; $n = 4$ slices from three animals), compared with 13% ± 4% of control with CPA ($P < 0.001$; $n = 6$ slices from five animals). (*B*) Consistent with partial inhibition of IP_3Rs by XC, GSK (100 nM) induced fast, high-amplitude "IP_3R-like" endfoot Ca^{2+} oscillations (blue trace) as well as slow, low-amplitude "TRPV4-like" oscillations (purple trace) similar to those seen in response to GSK with CPA present. In the presence of XC, GSK increased amplitude (*B*, *c*) of endfoot Ca^{2+} oscillations to 1.54 ± 0.40 $\Delta F/F_o$ ($P < 0.05$; $n = 4$ slices from three animals), but the effect on event frequency (*B*, *b*) did not reach significance ($n = 4$ slices from three animals). (*C*) Basal endfoot Ca^{2+} was not altered after 25 min of exposure to CPA ($n = 6$ slices from five animals). Values were compared by one-way ANOVA followed by Tukey's post hoc test (*A*) or by paired *t* test (*B* and *C*).

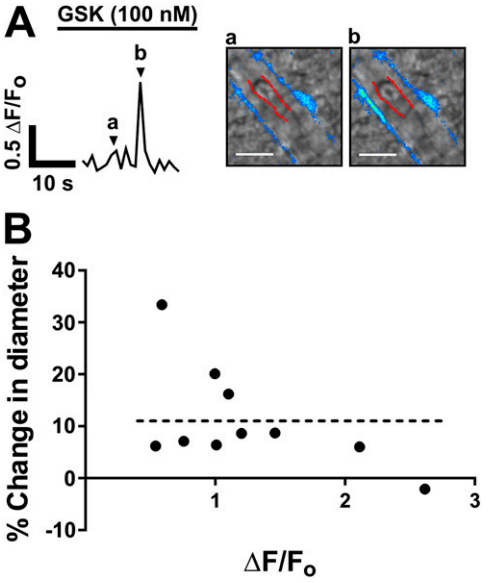

Fig. S4. Astrocytic endfoot Ca^{2+} oscillations induced by TRPV4 activation are associated with dilations of parenchymal arterioles in brain slices. (*A*) An endfoot Ca^{2+} oscillation stimulated by GSK transiently dilated the parenchymal arteriole (20%). (*B*) GSK-induced endfoot Ca^{2+} oscillations dilated parenchymal arterioles by an average of 11% ± 3% (indicated by the dashed line; $n = 10$ oscillations from six animals).

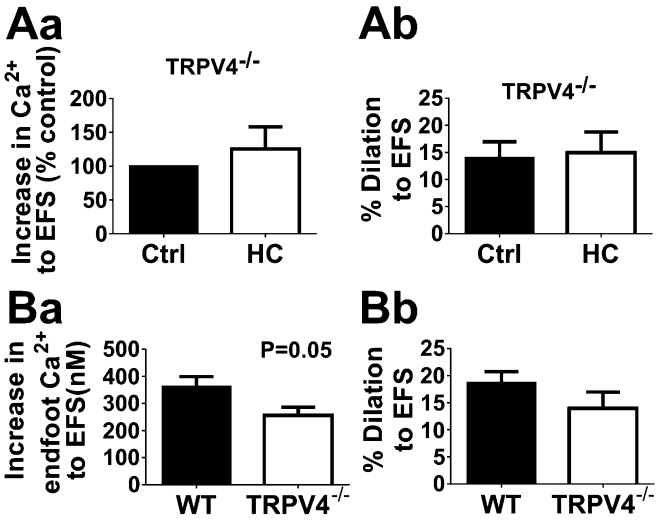

Fig. S5. TRPV4 inhibition with HC-067047 does not affect NVC responses in $TRPV4^{-/-}$ mice. (*A*) HC-067047 (10 μM) did not attenuate the increase in endfoot Ca^{2+} (*A*, *a*) or arteriolar dilation (*A*, *b*) to EFS in $TRPV4^{-/-}$ mice ($n = 7$ slices from three animals). (*B*) There was a trend toward a reduction in the EFS-induced increase in endfoot $[Ca^{2+}]_i$ (*B*, *a*) in $TRPV4^{-/-}$ compared with wild-type (WT) mice ($P = 0.05$), but arteriolar dilation (*B*, *b*) to EFS was not different in WT and $TRPV4^{-/-}$ mice ($n = 11$ for WT; $n = 8$ for $TRPV4^{-/-}$). Values in *A* were compared by paired *t* test; values in *B* were compared by unpaired *t* test.

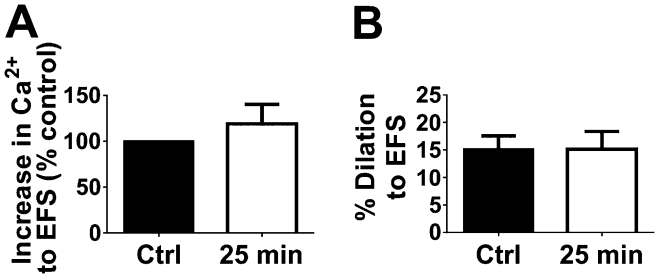

Fig. S6. NVC responses in brain slice experiments are unchanged over the course of 25 min. Time control experiments indicate that increases in endfoot Ca^{2+} (*A*) and arteriolar dilation (*B*) to EFS were unchanged after 25 min, the maximum incubation time used for pharmacological agents in comparisons of control and treatment conditions ($n = 4$ slices from four animals).

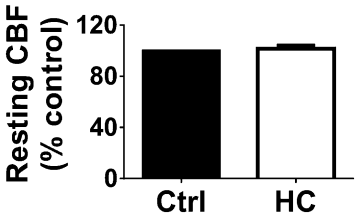

Fig. S7. Superfusion of HC-067047 (10 μM) over the cortical surface of the brain had no effect on resting CBF measured by laser Doppler flowmetry ($n = 7$).

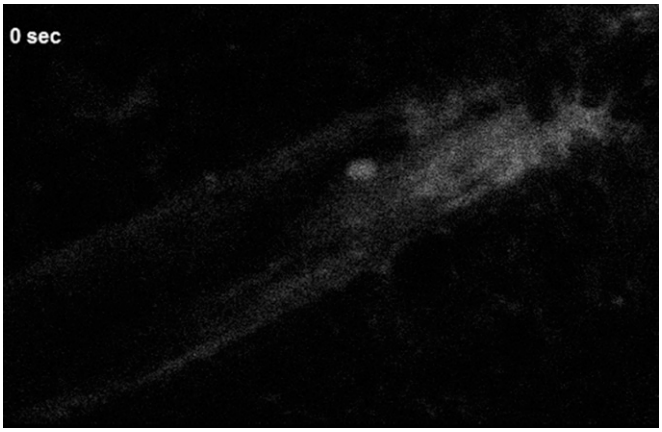

Movie S1. Astrocytic endfoot Ca^{2+} oscillations induced by the TRPV4 channel agonist, GSK (100 nM; 12× normal speed).

Movie S1

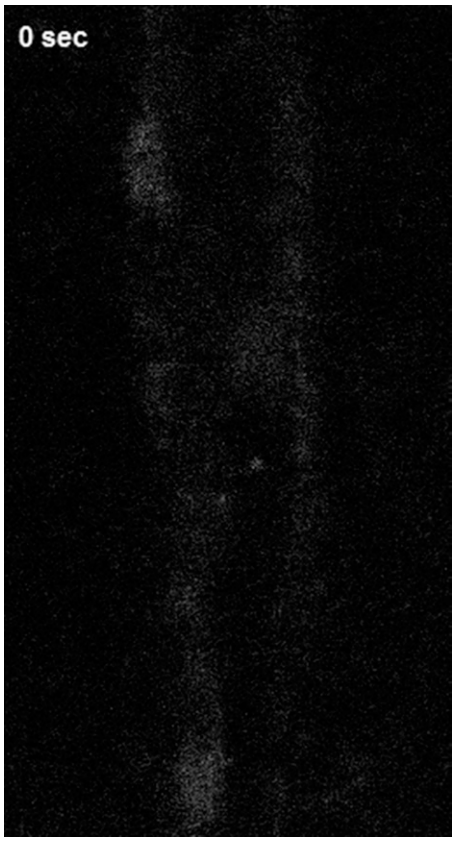

Movie S2. Astrocytic endfoot Ca^{2+} oscillations induced by 11,12-EET (1 μM; 12× normal speed).

Movie S2

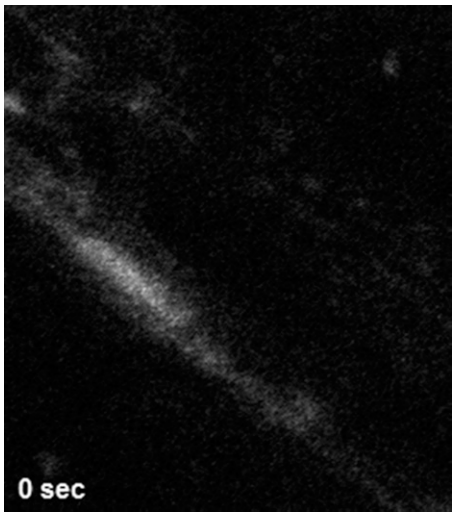

Movie S3. Astrocytic endfoot Ca^{2+} oscillations induced by GSK (100 nM) after depletion of ER Ca^{2+} stores with CPA (30 μM; 12× normal speed).

Movie S3

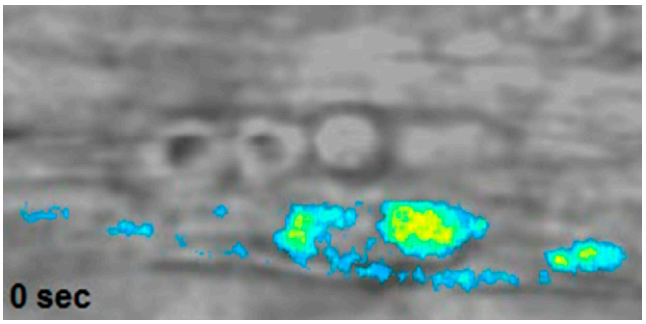

Movie S4. Control response of astrocytic endfoot $[Ca^{2+}]_i$ and parenchymal arteriolar diameter to EFS in the slice shown in Fig. 4 *A* and *B* (10× normal speed).

Movie S4

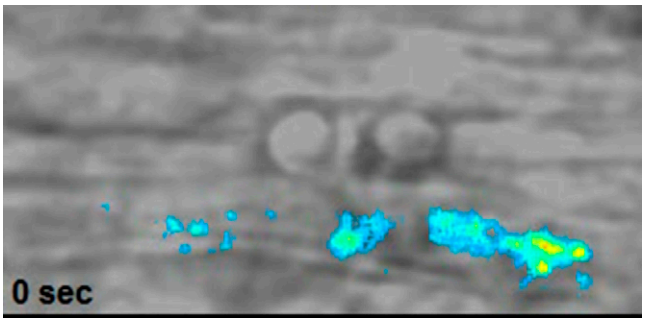

Movie S5. Response of astrocytic endfoot $[Ca^{2+}]_i$ and parenchymal arteriolar diameter to EFS after incubation with HC-067047 (10 μM) in the slice shown in Fig. 4 *A* and *B* (10× normal speed).

Movie S5